

# Refining time-space traffic diagrams: A multiple linear regression model

Zhengbing He\*

*Beijing Key Laboratory of Traffic Engineering, Beijing University of Technology, Beijing, China*

---

## Abstract

A time-space traffic (TS) diagram, which presents traffic states in time-space cells with color, is an important traffic analysis and visualization tool. Despite its importance for transportation research and engineering, most TS diagrams that have already existed or are being produced are too coarse to exhibit detailed traffic dynamics due to the limitations of existing information technology and traffic infrastructure investment. To increase the resolution of a TS diagram and enable it to present ample traffic details, this paper introduces the TS diagram refinement problem and proposes a multiple linear regression-based model to solve the problem. Two tests, which attempt to increase the resolution of a TS diagram 4 and 16 times, are carried out to evaluate the performance of the proposed model. Data collected at different times, in different locations and even in different countries are employed to thoroughly evaluate the accuracy and transferability of the proposed model. Strict tests with diverse data show that the proposed model, despite its simplicity, is able to refine a TS diagram with promising accuracy and reliable transferability. The proposed refinement model will “save” widely existing TS diagrams from their blurry “faces” and enable TS diagrams to show more traffic details.

*Keywords:* Superresolution, spatiotemporal speed contour diagrams, multiple linear regression, traffic dynamics, traffic state estimation

---

---

\*Corresponding author

*Email address:* he.zb@hotmail.com (Zhengbing He)

## 1. Introduction

A time-space traffic (TS) diagram, in which the x-axis indicates time, the y-axis denotes space, and a diverse array of colors represents different traffic states, is an important traffic analysis and visualization tool. From a TS diagram, we can identify traffic bottlenecks (Chen et al., 2004; Ban et al., 2008), understand traffic characteristics (Wan et al., 2020; He et al., 2015a), predict travel time (Ma et al., 2017; Zhang et al., 2017), and even estimate traffic emissions (He et al., 2020). Almost all traffic data centers and display platforms, such as California’s Performance Measurement System (PeMS) in the United States, employ TS diagrams to illustrate traffic dynamics.

Usually, a TS diagram is constructed by virtually partitioning a time-space plane into homogeneous cells and by filling the cells with colors that indicate traffic states (commonly represented by using traffic speed) in a TS diagram (He et al., 2019). The key step in constructing a TS diagram is to measure the speed that corresponds to each TS cell. Ideally, traffic speed can be accurately calculated by using 100% high-fidelity vehicle trajectories that pass through TS cells. Therefore, we could construct a high-resolution TS diagram with small cells to exhibit detailed traffic and to analyze traffic characteristics, such as stop-and-go waves and the fundamental diagram. Unfortunately, existing information technology does not support the wide collection of such 100% high-fidelity, vehicle trajectory data in practice, and we can only collect sampled traffic data for daily applications.

To derive the traffic speed in a specific TS cell using sampled data, traffic state estimation is usually needed. For example, given the loop detector data at two spatial locations, the intermediate traffic states can be estimated based on traffic characteristics (Treiber and Helbing, 2002; Treiber et al., 2011), the Kalman filter (Wang and Papageorgiou, 2005; Wang et al., 2007, 2008), Newell’s three-detector approach (Laval et al., 2012; Deng et al., 2013), etc. Given floating car data, traffic states can be approximated by mapping the data to carefully selected spatial cells that overlap a freeway (He et al., 2017; He and Liang, 2017). However, the loop detector density cannot be as high as we expected due to financial limitations (?). For example, the detector spacing is usually between several hundred meters and several kilometers. The interval that aggregates the uploaded loop detector data cannot be too short, limited by transmission bandwidth and storage space; it is common to set the time interval of uploading detector

data to 1 min to 10 min. For similar reasons, the sampling rate and penetration rate of floating car data are usually low in practice, and it is quite typical for a floating car to upload its driving status data every 1 minute or an even longer duration. The sparse nature of time-space sampled data make it difficult to construct a high-resolution TS diagram even with the aid of advanced traffic state estimation methods.

To extract more traffic details from a widely existing, low-resolution TS diagram, a meaningful and interesting attempt is to directly refine a TS diagram and increase its resolution. In computer science, this approach is referred to as *superresolution*, i.e., enhancing the resolution of an imaging system (Tsai and Huang, 1984; Irani and Peleg, 1990). Superresolution is an active field, particularly with the development of deep-learning approaches (Wang et al., 2015; Dong et al., 2016; Zhang et al., 2018). Convolutional neural networks (CNNs) are the most popular foundation of various deep learning-based supersolution approaches due to their powerful capability of processing images (Wu et al., 2021). Machine learning-based supersolution approaches do not require solving complex equations, and the drawbacks of these approaches are twofold. First, the computational cost is usually high, hindering the real-time applications of supersolution approaches (Wu et al., 2021). Second, a large number of images are needed for training deep-learning models (Zhang et al., 2022). For the purpose of refining a TS diagram in transportation, the second drawback is a major barrier, i.e., it is unrealistic to collect high-fidelity and high-sampling-rate traffic data as we previously mentioned, and thus, we do not have enough target images to train deep-learning models.

In summary, the resolution of most TS diagrams that have already existed or are being generated is quite coarse for a detailed analysis and applications, mainly limited by existing information technology and traffic infrastructure investment. Since a TS diagram is one of the most important traffic analysis and visualization tools, a method that could increase the resolution of TS diagrams without a large number of high-resolution TS diagrams for model training is urgently needed. With such a method, widely existing TS diagrams could be “saved” from their blurry “faces”. To fill this gap, this paper proposes a multiple linear regression-based model to refine a low-resolution TS diagram so that a high-resolution TS diagram with ample traffic details, such as traffic waves, can be derived from the diagram. To the best of our knowledge, this is

the first work that introduces the refinement problem of a TS diagram and successfully solves it with only a small amount of high-fidelity traffic data.

The remainder of the paper is organized as follows: Section 2 introduces the refinement problem of a TS diagram and proposes a refinement model based on multiple linear regression. Section 3 evaluates the proposed refinement model using three completely different datasets in two strict tests. The discussion and conclusion are presented in Sections 4 and 5, respectively.

## 2. Model

*Refinement problem of a TS diagram. Given the traffic speed of a cell in a TS diagram, partition the cell into four homogenous subcells and estimate the traffic speed of the four subcells to achieve the goal of refining a given TS diagram by increasing its resolution (refer to Figure 1).*

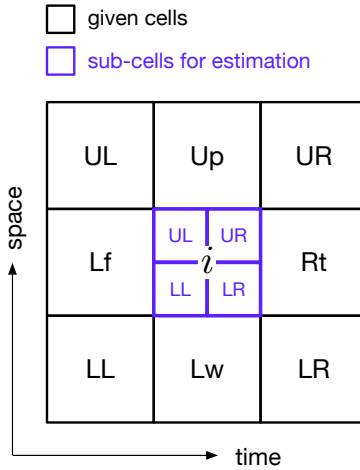


Figure 1: Schematic of the refinement of a TS diagram.  $i$ : the cell to be refined; LL: lower-left; Lw: lower; LR: lower-right; Rt: right; UR: upper-right; Up: upper; UL: upper-left; Lf: left.

Let  $i$  and  $x_i$  be a TS cell and its corresponding average speed, respectively. Partition Cell  $i$  into four homogenous TS subcells and denote by  $y_i^j$  and  $\hat{y}_i^j$  the ground-truth and estimated speeds, respectively, of Subcell  $j$  of Cell  $i$ , where  $j \in \mathbf{J} = \{\text{LL}, \text{LR}, \text{UR}, \text{UL}\}$  represents the lower-left (LL), lower-right (LR), upper-right (UR) and upper-low (UL) subcells of Cell  $i$ , respectively (Figure 1).

It is well known that there are two traffic conditions with different propagation directions of waves, i.e., the free-flow condition where traffic waves propagate forward and the congested condition where traffic waves propagate backward (Figure 2). The

opposite propagation directions of traffic waves have a distinguishing impact on traffic state estimation; thus, traffic conditions should be taken into account to properly capture the fundamental characteristics of traffic.

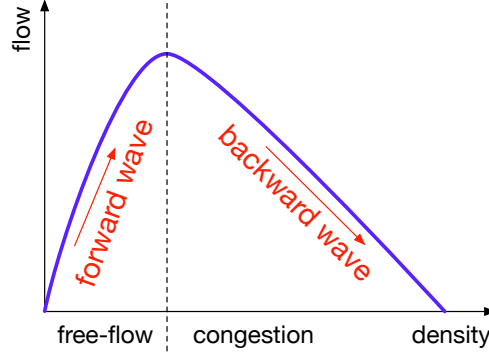


Figure 2: Fundamental diagram of traffic and traffic waves.

To solve the refinement problem, we involve the cells that surround Cell  $i$  and propose a multiple linear regression-based refinement model to calculate  $\hat{y}_i^j$  as follows:

$$\hat{y}_i^j = \mathbf{p}^{jk} \cdot \mathbf{x}_i + \varepsilon^{jk} \quad (1)$$

where

$$\mathbf{x}_i = [x_i, x_{LL}, x_{Lw}, x_{LR}, x_{Rt}, x_{UR}, x_{Up}, x_{UL}, x_{Lf}] \quad (2)$$

where  $x_{LL}$ ,  $x_{Lw}$ ,  $x_{LR}$ ,  $x_{Rt}$ ,  $x_{UR}$ ,  $x_{Up}$ ,  $x_{UL}$  and  $x_{Lf}$  are the ground-truth average speeds of the LL, lower (Lw), LR, right (Rt), UR, upper (Up), UL and left (Lf) cells surrounding Cell  $i$ , respectively. The corresponding parameters of  $\mathbf{x}_i$  are

$$\mathbf{p}^{jk} = [p^{jk}, p_{LL}^{jk}, p_{Lw}^{jk}, p_{LR}^{jk}, p_{Rt}^{jk}, p_{UR}^{jk}, p_{Up}^{jk}, p_{UL}^{jk}, p_{Lf}^{jk}] \quad (3)$$

and  $\varepsilon^{jk}$  is a constant, where  $k \in \{\text{ff}, \text{cg}\}$  indicates the free-flow (ff) and congested (cg) conditions of Cell  $i$ . According to the basic knowledge of traffic flow theory and real-world traffic characteristics, the speed threshold  $x^* = 60$  km/h is employed to distinguish the free-flow and congested traffic conditions of Cell  $i$ , i.e., the traffic is in the free-flow condition when  $x_i < x^*$ ; otherwise, the traffic is in the congested condition.

To obtain the ground-truth values  $\mathbf{x}_i$  and  $y_i^j$ , we employ vehicle trajectory data on a freeway segment and construct TS diagrams with various cell sizes. To derive the

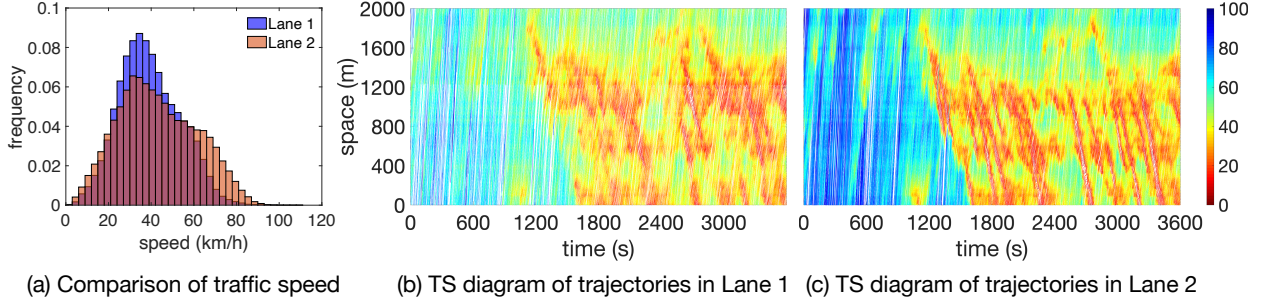


Figure 3: Summary of the 1-hour trajectory data (No. F001) for Ikeda-Route-11 of the Japanese ZenTraffic dataset.

values of parameters  $\mathbf{p}^{jk}$ , we fit the data to Equation 1 using the least squares method.

This paper employs 1-hour, 2-lane trajectory data (No. F001) contained in the Ikeda-Route-11 dataset of the open-source ZenTraffic dataset (Hanshin Exp. Co. Ltd., 2018; Dahiya et al., 2020) to estimate the model parameters in Equation 1. The data were collected in 2017 on a two-lane freeway segment of Ikeda Route 11 in Japan. The length of the segment is 2 km, and the total duration of data collection is 5 hours (No. F001-F005). The first hour of data (i.e., No. F001) are used to estimate the parameters in this section, and the remaining 4 hours of data (i.e., No. F002-F005) are used to validate the model in Section 3. As shown in Figure 3, the 1-hour data contain both free-flow traffic and congested traffic with typical traffic characteristics, such as stop-and-go waves. It is also observed that the maximum speed in Lane 2 (approximately 90 km/h) is slightly higher than that in Lane 1 (approximately 70 km/h). Generally, the data is qualified for model fitting.

The parameter estimation results of the proposed refinement model with respect to different cell sizes are presented in Table 1. It can be seen that all  $R^2$ , i.e., coefficient of determination, are greater than 0.75. In particular,  $R^2$  for estimating the parameters in the congested condition are greater than 0.9. This is quite a satisfactory result for an empirical study.

### 3. Model evaluation

To avoid the autocorrelation of data and to fairly test the model (Equation 1 and Table 1), we employ data collected from completely different freeway segments, one of which is even located in another country. This setting could well demonstrate the

Table 1: Parameters of the refinement model that are estimated using the following data: Ikeda-Route-11 F001, lanes 1 and 2, ZenTraffic dataset, Japan.

Cell size	Sub-cell				Estimated parameters of Equation 1										$R^2$
	size	$k$	$j$	#	$p_C^{jk}$	$p_{LL}^{jk}$	$p_{Lw}^{jk}$	$p_{LR}^{jk}$	$p_{Rt}^{jk}$	$p_{UR}^{jk}$	$p_{Up}^{jk}$	$p_{UL}^{jk}$	$p_{Lf}^{jk}$	$\epsilon^{jk}$	
30s × 50m	15s ×	ff	LL	2305	0.95	0.43	-0.28	0.02	0.13	-0.27	0.31	-0.11	-0.20	0.84	<b>0.8170</b>
			LR	2302	0.88	-0.38	0.66	-0.12	-0.03	0.25	-0.54	0.06	0.22	0.30	<b>0.8435</b>
	25m		UR	2303	1.06	-0.40	0.35	-0.01	-0.26	0.34	-0.32	0.08	0.16	-0.13	<b>0.8489</b>
			UL	2306	0.83	0.30	-0.51	0.03	0.16	-0.25	0.60	-0.19	0.04	0.66	<b>0.8171</b>
	cg	LL	7257	0.97	-0.08	-0.09	-0.01	-0.17	0.00	0.09	0.05	0.23	0.19	<b>0.9716</b>	
		LR	7258	0.99	0.07	-0.20	-0.00	0.21	-0.02	0.20	-0.10	-0.16	0.06	<b>0.9704</b>	
		UR	7258	0.95	0.03	0.14	0.05	0.19	-0.06	-0.08	-0.01	-0.22	0.41	<b>0.9710</b>	
		UL	7257	0.92	-0.00	0.21	-0.06	-0.19	0.09	-0.20	0.01	0.20	0.43	<b>0.9713</b>	
60s × 100m	30s ×	ff	LL	532	1.13	0.41	-0.28	0.02	0.01	-0.15	0.14	-0.06	-0.21	-0.75	<b>0.8585</b>
			LR	532	0.62	-0.39	0.69	-0.07	0.08	0.11	-0.34	-0.01	0.27	3.65	<b>0.8587</b>
	50m		UR	532	0.86	-0.41	0.36	-0.05	-0.02	0.15	-0.15	0.04	0.19	2.38	<b>0.8636</b>
			UL	532	1.13	0.39	-0.63	0.09	-0.05	-0.10	0.41	-0.10	-0.12	-1.50	<b>0.8671</b>
	cg	LL	1764	1.02	-0.06	-0.03	-0.09	-0.09	0.01	-0.01	0.14	0.10	0.90	<b>0.9502</b>	
		LR	1764	0.89	0.06	-0.24	0.05	0.17	-0.06	0.32	-0.17	-0.03	0.86	<b>0.9517</b>	
		UR	1764	1.04	0.05	0.02	0.16	0.05	-0.03	-0.04	-0.09	-0.14	-0.03	<b>0.9520</b>	
		UL	1764	0.87	-0.05	0.33	-0.12	-0.08	0.07	-0.27	0.08	0.16	0.52	<b>0.9491</b>	
120s × 200m	60s ×	ff	LL	118	1.08	0.14	-0.05	0.01	-0.15	-0.03	0.07	-0.08	-0.07	5.49	<b>0.7952</b>
			LR	118	0.58	-0.20	0.53	-0.08	0.18	0.08	-0.30	0.07	0.18	-1.18	<b>0.7963</b>
	50m		UR	118	0.75	-0.07	0.15	-0.07	0.19	0.04	-0.01	0.12	-0.06	-1.96	<b>0.7616</b>
			UL	118	1.26	0.11	-0.38	0.12	-0.22	-0.05	0.21	-0.02	-0.06	1.87	<b>0.7812</b>
	cg	LL	404	1.04	-0.03	-0.06	-0.13	-0.04	-0.08	0.00	0.21	0.06	0.97	<b>0.9277</b>	
		LR	404	0.93	0.07	-0.31	0.14	0.10	-0.03	0.31	-0.16	-0.04	0.57	<b>0.9261</b>	
		UR	404	1.07	0.05	0.02	0.23	-0.08	0.10	-0.10	-0.15	-0.13	0.26	<b>0.9293</b>	
		UL	404	0.83	-0.08	0.40	-0.19	-0.01	0.03	-0.27	0.10	0.17	0.88	<b>0.9246</b>	
240s × 400m	120s ×	ff	LL	19	0.27	-0.05	0.21	0.21	-0.06	-0.01	0.45	-0.38	0.38	0.14	<b>0.8752</b>
			LR	19	-0.46	-0.49	1.46	-0.46	0.51	-0.76	0.38	0.29	0.50	-2.13	<b>0.8339</b>
	100m		UR	19	0.71	-0.40	0.33	-0.28	0.24	-0.18	0.24	0.36	0.05	-3.23	<b>0.8273</b>
			UL	19	2.54	0.48	-1.38	0.43	-0.51	0.70	-0.61	-0.26	-0.39	1.88	<b>0.8602</b>
	cg	LL	85	0.97	-0.06	0.13	-0.11	0.03	0.04	-0.02	0.03	0.09	-1.88	<b>0.9344</b>	
		LR	85	0.82	-0.03	-0.26	0.02	0.10	-0.04	0.44	-0.22	0.16	-0.76	<b>0.9514</b>	
		UR	85	1.37	0.10	-0.29	0.29	-0.23	0.06	-0.30	0.08	-0.18	4.32	<b>0.9266</b>	
		UL	85	0.76	-0.01	0.47	-0.22	0.08	-0.10	-0.03	0.09	-0.03	-0.49	<b>0.9353</b>	

performance of the proposed model and guarantee a high reliability of evaluation.

### 3.1. Data

To thoroughly evaluate the model performance, we employ the following three high-fidelity, vehicle trajectory datasets.

- *Different-time data.* The other 4-hour 2-lane vehicle trajectory data (i.e., No. F002-F005) in the Ikeda-Route-11 dataset of the ZenTraffic dataset in Japan ([Hanshin Exp. Co. Ltd., 2018](#); [Dahiyal et al., 2020](#)).
- *Different-location data.* The 5-hour, 2-lane vehicle trajectory data (i.e., No. F001-F005) in the Wangan-Route-4 dataset of the ZenTraffic dataset in Japan ([Hanshin Exp. Co. Ltd., 2018](#); [Dahiyal et al., 2020](#)). The Wangan-Route-4 dataset is another high-fidelity trajectory dataset contained in the ZenTraffic dataset. The data were collected on a 1.6 km, 2-lane freeway segment in Wangan Route 4 in Japan, and the duration of data collection was 5 hours in total.
- *Different-country data.* The 45-minute, 5-lane trajectory vehicle data of the US-101 dataset were provided by the Next Generation Simulation (NGSIM) program ([U.S. Federal Highway Administration, 2006](#)). The well-known US-101 dataset was collected on a 640 m, 5-lane segment in the vicinity of Lankershim Avenue on the southbound US-101 freeway in Los Angeles, California, from 7:50 a.m. to 8:35 a.m. on June 15, 2005.

It is believed that the three datasets could guarantee the reliability of the evaluation results based on the following two facts. First, the three datasets include traffic data collected at different times, in different locations and even in different countries<sup>1</sup>, which differ from the data employed for model estimation. Diverse and abundant traffic patterns are observed. Second, the three datasets cover a total of 4.24 km segments, a 9.75 h collection duration and a total of 9 lanes (Table 2). Such a large spatiotemporal range of the data ensures the sufficiency of the evaluation.

---

<sup>1</sup>It is even left-hand traffic in Japan, which is quite different from the traffic in the United States.

Table 2: Attributes of the trajectory datasets utilized for model estimation and evaluation.

	Dataset	Segment length (km)	Collection duration (h)	Lane #	Country
Estimation	Ikeda-Route-11	2	1 (F001)	2	Japan
Evaluation	Ikeda-Route-11	2	4 (F002-F005)	2	Japan
	Wangan-Route-4	1.6	5 (F001-F005)	2	Japan
	US-101	0.64	0.75 (7:50-8:35)	5	United States
	<b>Total</b>	<b>4.24</b>	<b>9.75</b>	<b>9</b>	

### 3.2. Measures of errors

To reflect the accuracy of the refinement, the following measures of errors are employed.

- Mean Absolute Error:

$$\text{MAE} = \frac{1}{N|\mathbf{J}|} \sum_{i=1}^N \sum_{j \in \mathbf{J}} |y_i^j - \hat{y}_i^j| \quad (4)$$

where  $|\mathbf{J}|$  is the size of set  $\mathbf{J}$  and  $|\mathbf{J}| = 4$ .

- Mean Absolute Percentage Error:

$$\text{MAPE} = \frac{1}{N|\mathbf{J}|} \sum_{i=1}^N \sum_{j \in \mathbf{J}} \left| \frac{y_i^j - \hat{y}_i^j}{y_i^j} \right| \quad (5)$$

### 3.3. Evaluation: 1-4 test

To validate the proposed refinement model, we first conduct a “1-4 test” as follows: *Given a TS cell, we estimate the traffic speed of its 4 homogenous subcells so that the resolution of the corresponding TS diagram is increased 4 times.*

Table 3 presents the results. It can be seen that all MAPEs are less than 0.1, even for the data collected from another country (i.e., US-101 dataset), and many of the MAPEs are even less than 0.05. The results demonstrate that the proposed model achieves high refinement accuracy in the 1-4 test. In addition, it is also observed that the refinement errors increase with the enlargement of the cells of the TS diagram to be refined. The reason is easy to understand, i.e., the larger the initial TS cells are, the more traffic

information is lost in the construction of the initial TS diagram, and thus, it is more difficult to obtain an accurate refinement.

Table 3: Results of model evaluation: 1-4 test.

Cell size	1-4 sub-cell		Ikeda-Route-11 (F002-F005)			Wangan-Route-4 (F001-F005)			US-101		
	size	$j$	Sub-cell #	MAE	MAPE	Sub-cell #	MAE	MAPE	Sub-cell #	MAE	MAPE
30s	15s	LL	38028	1.915	<b>0.040</b>	36941	1.603	<b>0.032</b>	4894	2.158	<b>0.086</b>
	×	LR	38035	1.911	<b>0.040</b>	36948	1.601	<b>0.032</b>	4894	2.157	<b>0.085</b>
50m	25m	UR	38025	1.904	<b>0.040</b>	36946	1.609	<b>0.032</b>	4894	2.144	<b>0.080</b>
		UL	38025	1.919	<b>0.041</b>	36947	1.611	<b>0.032</b>	4894	2.211	<b>0.085</b>
60s	30s	LL	9153	2.292	<b>0.050</b>	8790	1.911	<b>0.039</b>	1100	2.823	<b>0.098</b>
	×	LR	9153	2.267	<b>0.050</b>	8790	1.929	<b>0.040</b>	1100	2.748	<b>0.093</b>
100m	50m	UR	9153	2.229	<b>0.049</b>	8790	1.925	<b>0.039</b>	1100	2.754	<b>0.095</b>
		UL	9153	2.301	<b>0.049</b>	8790	1.947	<b>0.039</b>	1100	2.927	<b>0.099</b>
120s	60s	LL	2088	2.783	<b>0.061</b>	1974	2.228	<b>0.046</b>	—	—	—
	×	LR	2088	2.781	<b>0.063</b>	1974	2.242	<b>0.047</b>	—	—	—
200m	100m	UR	2088	2.660	<b>0.061</b>	1974	2.243	<b>0.044</b>	—	—	—
		UL	2088	2.782	<b>0.061</b>	1974	2.232	<b>0.044</b>	—	—	—
240s	120s	LL	416	3.316	<b>0.073</b>	390	2.916	<b>0.058</b>	—	—	—
	×	LR	416	4.431	<b>0.085</b>	390	4.543	<b>0.084</b>	—	—	—
400m	200m	UR	416	3.634	<b>0.077</b>	390	3.419	<b>0.062</b>	—	—	—
		UL	416	4.434	<b>0.085</b>	390	4.298	<b>0.079</b>	—	—	—

Note: the length of the segment where the US-101 dataset was collected is not enough for the test with cell sizes 120s × 200m and 240s × 400m.

### 3.4. Evaluation: 1-4-16 test

Furthermore, we conduct a stricter “1-4-16 test” as follows: *Given a TS cell, we estimate the traffic speed of its homogenous 4 subcells (referred to as 1-4 subcells) and further estimate the traffic speed of the homogenous 4 subcells (referred to as 4-16 subcells) of each of the 1-4 subcells by using the estimated speed of these 1-4 subcells. In the test, the resolution of a given TS diagram will be increased 16 times.* Note that when estimating the traffic speed of 4-16 subcells, we only input the estimated speed of 1-4 subcells, meaning that in the 1-4-16 test, the only input data consists of the speeds of the TS cells in the initial TS diagram.

Table 4 presents the results, from which the following observations can be made: All MAPEs are less than 0.17, and many MAPEs are less than 0.1. Compared with the 1-4 test, increasing the resolution 16 times indeed results in more errors, whereas the magnitude of the errors is acceptable. In general, the estimation results are satisfactory, particularly for a study that is based on empirical data.

Table 4: Results of model evaluation: 1-4-16 test.

Cell size	1-4-16 sub-cell		Ikeda-Route-11 (F002-F005)			Wangan-Route-4 (F001-F005)			US-101		
	size	$j$	Sub-cell #	MAE	MAPE	Sub-cell #	MAE	MAPE	Sub-cell #	MAE	MAPE
60s	15s	LL	31994	3.195	<b>0.070</b>	29893	2.606	<b>0.054</b>	3006	3.804	<b>0.160</b>
	×	LR	31987	3.218	<b>0.073</b>	29899	2.658	<b>0.055</b>	3006	3.787	<b>0.158</b>
100m	25m	UR	31987	3.218	<b>0.073</b>	29897	2.605	<b>0.053</b>	3006	3.783	<b>0.153</b>
		UL	31990	3.240	<b>0.072</b>	29897	2.611	<b>0.053</b>	3006	3.894	<b>0.155</b>
120s	30s	LL	6272	3.953	<b>0.093</b>	5440	3.130	<b>0.065</b>	—	—	—
	×	LR	6272	3.941	<b>0.097</b>	5440	3.110	<b>0.066</b>	—	—	—
200m	50m	UR	6272	3.813	<b>0.091</b>	5440	2.923	<b>0.061</b>	—	—	—
		UL	6272	3.894	<b>0.090</b>	5440	3.058	<b>0.063</b>	—	—	—
240s	60s	LL	768	5.808	<b>0.132</b>	480	4.002	<b>0.085</b>	—	—	—
	×	LR	768	7.720	<b>0.160</b>	480	6.134	<b>0.122</b>	—	—	—
400m	100m	UR	768	6.254	<b>0.137</b>	480	4.776	<b>0.098</b>	—	—	—
		UL	768	7.988	<b>0.166</b>	480	6.093	<b>0.120</b>	—	—	—

Note: the length of the segment where the US-101 dataset was collected is not enough for the test with cell sizes 120s  $\times$  200m and 240s  $\times$  400m.

To visually present the results, we illustrate an example of the 1-4 and 1-4-16 tests in Figure 4. It is impressive to discover that a TS diagram with quite coarse traffic patterns (Figure 4(b1)) can be refined to a TS diagram, where even detailed stop-and-go waves can be observed (Figure 4(b3)). Moreover, in the low-resolution TS diagram (Figure 4(b1)), the traffic propagation directions are almost vertical. After the refinement, the propagation directions with slopes are clearly revealed in Figures 4(b3) and 4(c2), which is more consistent with the real-world traffic patterns (Figures 4(a) and 4(d)). Compared with the ground-truth diagram (Figure 4(d)), both the refined TS diagrams in the 1-4 and 1-4-16 tests (Figures 4(c2) and 4(b3)) satisfactorily reproduce the details of traffic patterns such as stop-and-go waves and wave directions. Generally, the visual comparison clearly demonstrates the power of the proposed refinement model.

Table 4 also shows that the MAPEs for refining the diagram constructed using the US-101 dataset are slightly greater than those of the other diagrams. We discuss the following reasons: In comparison, the MAEs for refining the US-101 diagram are not significantly greater than those of the other diagrams, indicating that the high MAPEs partially result from the lower ground-truth traffic speed that is contained by the US-101 dataset (i.e., a smaller  $y_i^j$  will increase the MAPE according to Equation 5). In addition, there might still be certain differences between the traffic patterns of two

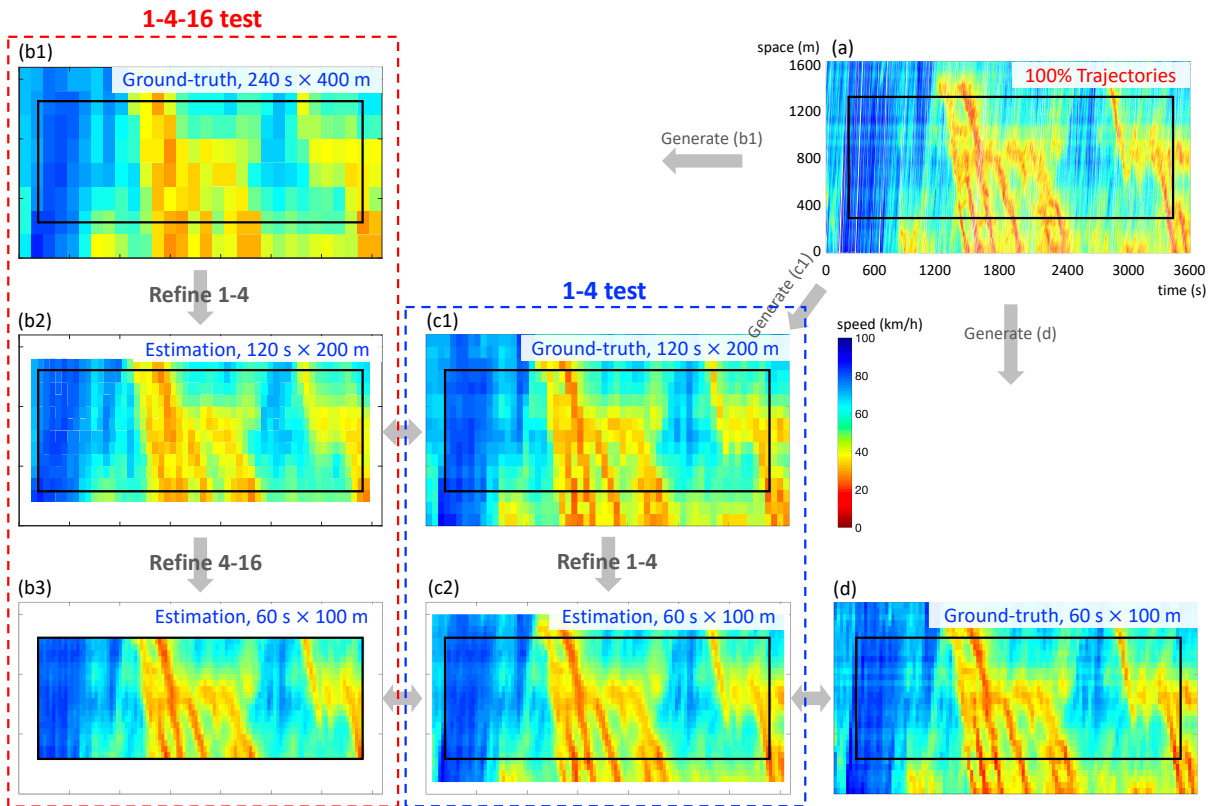


Figure 4: Visual presentation of the 1-4 test (red dashed box) and the 1-4-16 test (blue dashed box) with a selected example. *Target data*: Wangan-Route-4, F003, Lane 2. *1-4-16 test*: Refining a TS diagram from  $240\text{ s} \times 400\text{ m}$  cells to  $60\text{ s} \times 100\text{ m}$  cells, i.e., increasing the resolution 16 times. *1-4 test*: Refining a TS diagram from  $120\text{ s} \times 200\text{ m}$  cells to  $60\text{ s} \times 100\text{ m}$ , i.e., increasing the resolution 4 times. Note that the edge of a TS diagram cannot be refined since the surrounding cells have to be taken as the input data. Therefore, the resulting TS diagram is smaller in size than the initial diagram. For convenience in our comparison, we add a black box to each diagram to indicate the resulting region in the 1-4-16 test (b3).

different countries or among the specific segments of data collection. The existence of errors is understandable, and the magnitude is acceptable.

We supplement Figure 5 to visually show the details of the refinement results of the US-101 diagram in the 1-4-16 test. The main traffic pattern is well retained in the  $15\text{ s} \times 20\text{ m}$  TS diagram (Figure 5(b)) that is refined from the  $60\text{ s} \times 100\text{ m}$  TS diagram (Figure 5(a)) compared with the ground-truth TS diagram in Figure 5(c). Figure 5(d), which presents the speed changes for a specific location in the TS diagrams, further supports the judgment, i.e., the speed changes of the refined TS diagram (red line) generally overlap those of the ground-truth diagram (blue line), and it shows a clearer up-and-down trend, i.e., stop-and-go waves, compared with that in the original TS diagram with lower resolution (green line). Moreover, as indicated by the circles in Figures 5(b) and 5(c), the refined TS diagram fails to capture sufficient detail in traffic propagation. This lack of detail might be attributed to the notion that the small amount of detail has already been omitted when constructing the initial low-resolution, TS diagram (refer to the circled area in Figure 5(a)), making it very difficult or even impossible to reproduce more details.

#### 4. Discussion

We choose a linear regression method, which is simple in form, as the foundation of modeling based on the following considerations. First, as we have carefully shown, the simple method is able to achieve high goodness of fits (Table 1) and make satisfactory refinement, even for estimating the TS diagram from another country (Table 3) as well as in the stricter 1-4-16 test (Table 4 and Figure 4). Achieving good results is the ultimate goal for a study that aims to solve a problem instead of proposing an advanced method. Second, a linear regression method could give a distinct expression that is simply contained in Table 1; it is very convenient for spread and applications in practice. We could obtain the dominant impact factors from the parameter values. Notably, there are many powerful machine learning methods in the era of big data and machine learning. One could try to solve the problem by proposing a machine learning-based method; it is an interesting future direction of this study. However, the limited number of samples for training is still a major barrier for these methods to overcome.

Similarly, the contribution of the study is to introduce the new problem of refin-

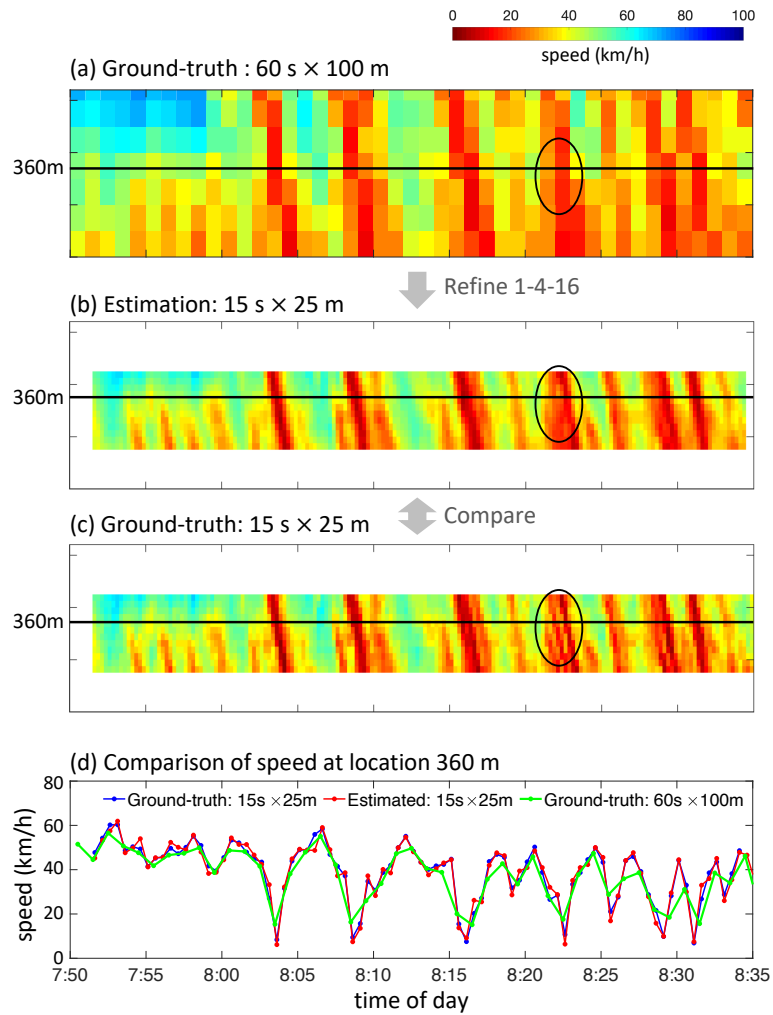


Figure 5: 1-4-16 test of the 60 s × 100 m TS diagram constructed using the US-101 Lane-2 data. (a) Ground-truth 60 s × 100 m TS diagram for refinement; (b) 1-4-16 refined 15 s × 25 m TS diagram; (c) Ground-truth TS diagram corresponding to the refined diagram in (b); (d) Comparison of the time series of traffic speeds at location 360 m.

ing TS diagrams and then effectively solving it, instead of proposing a more advanced method to solve an existing problem. To the best of our knowledge, there is no comparative method, and thus, we cannot make a comparison with other methods.

In a regression analysis, usually only one of the highly correlated variables are retained to avoid multicollinearity. However, in the refinement problem of this paper, all variables, i.e., the speeds of the 9 cells in Figure 1, might be highly correlated due to the spatiotemporal closeness of these cells, and any of them is highly likely to influence details of the refinement. Therefore, we could not discard any of them to achieve a high prediction accuracy, particularly to capture important traffic patterns, such as the directions of traffic waves.

Moreover, we believe that the proposed refinement model has good transferability. First, good transferability has been demonstrated in the test with data collected at different times, in different locations and even in different countries. Second, beyond adding new tests, good transferability could be guaranteed by the traffic itself, i.e., it is well known that traffic shows similar and limited patterns worldwide; for example, the backward wave speed is globally observed between -20 and -10 km/h, and the period of the stop-and-go wave ranges from 2 to 15 min (Zielke et al., 2008; Laval and Leclercq, 2010; Chen et al., 2012; Jiang et al., 2014; He et al., 2015b). Thus, it is highly possible to predict traffic at other times and places by simply inputting typical traffic patterns.

Distinguishing free-flow and congested traffic conditions is indispensable for the proposed refinement model. In the preliminary stage of the study, we did not distinguish among the conditions and failed to capture the forward waves in free-flow traffic (i.e., we do not observe free-flow waves toward the top right corner in, e.g., Figure 4(c2)), although a high goodness of fit could also be achieved.

## 5. Conclusion

To increase the resolution of widely-existing coarse TS diagrams and to make them exhibit more detailed traffic dynamics, this paper introduces a TS diagram refinement problem for the first time and proposes a multiple, linear regression-based refinement model (Equation 1 and Table 1) to solve the problem. The TS diagrams with 4 different cell sizes, i.e.,  $30\text{ s} \times 50\text{ m}$ ,  $60\text{ s} \times 100\text{ m}$ ,  $120\text{ s} \times 200\text{ m}$  and  $240\text{ s} \times 400\text{ m}$ , are selected

as examples and considered in the model. Three datasets are employed to propose and evaluate the model, i.e., the Ikeda-Route-11 dataset in Japan, the Wangan-Route-4 dataset in Japan, and the US-101 datasets in the United States (Table 2). In parameter estimation, the proposed model achieves a high goodness of fit with  $R^2 > 0.7$  in the free-flow traffic condition and  $R^2 > 0.9$  in the congested traffic condition (Table 1). The 1-4 and 1-4-16 tests are then conducted to evaluate the accuracy and transferability of the proposed refinement model. The 1-4 test refines a TS diagram by increasing the resolution 4 times, and the 1-4-16 test is a stricter test for increasing the resolution 16 times. Remarkably, the model shows satisfactory small prediction errors in the tests, i.e., The ranges of the MAE and MAPE in the 1-4 test are (1.6 5) and (0.03 0.1), respectively (Table 3); The ranges of the MAE and MAPE in the 1-4-16 test are (2.5 8) and (0.05 0.17), respectively (Table 4). A visual presentation of the refinement results of the two tests (Figures 4 and 5) is further made to better illustrate the effectiveness of the proposed model. Moreover, the source of error is carefully analyzed, and it is determined that some very detailed traffic dynamics that have been omitted from the initial low-resolution TS diagram are more difficult to reproduce in a refinement. The sufficient tests and high accuracy of refinement persuasively demonstrate the effectiveness of the proposed refinement model, although it is simple in model form.

We believe that the proposed refinement model is rather significant after considering the importance and wide-existence of TS diagrams in transportation research and engineering. It would be a powerful tool that could quickly and effectively “clean” coarse TS diagrams and enable them to exhibit ample traffic details. Further improving the refinement accuracy and reproducing more omitted details will be a meaningful future research direction. Incorporating more knowledge of traffic flow theory and characteristics may be essential and helpful. Moreover, deep learning provides us with fruitful and capable tools that might have the potential to make breakthroughs feasible. However, the strategy for introducing a deep-learning method should be tactical since high-fidelity traffic data that could be used for model training are usually very limited.

## Acknowledgment

The research is funded by National Natural Science Foundation of China (71871010).

## References

- Ban, X.J., Chu, L., Benouar, H., 2008. Bottleneck Identification and Calibration for Corridor Management Planning. *Transportation Research Record: Journal of the Transportation Research Board* 1999, 40–53.
- Chen, C., Skabardonis, A., Varaiya, P., 2004. Systematic Identification of Freeway Bottlenecks. *Transportation Research Record: Journal of the Transportation Research Board* 1867, 46–52.
- Chen, D., Laval, J., Ahn, S., Zheng, Z., 2012. Microscopic traffic hysteresis in traffic oscillations: A behavioral perspective. *Transportation Research Part B: Methodological* 46, 1440–1453.
- Dahiyal, G., Asakura, Y., Nakanishi, W., 2020. A study of speed-density functional relations for varying spatiotemporal resolution using Zen Traffic Data, in: *23rd IEEE International Conference on Intelligent Transportation Systems (ITSC)*.
- Deng, W., Lei, H., Zhou, X., 2013. Traffic state estimation and uncertainty quantification based on heterogeneous data sources: A three detector approach. *Transportation Research Part B: Methodological* 57, 132–157.
- Dong, C., Loy, C.C., He, K., Tang, X., 2016. Image super-resolution using deep convolutional networks. *IEEE Transactions on Pattern Analysis and Machine Intelligence* 38, 295–307.
- Hanshin Exp. Co. Ltd., 2018. Zen Traffic Data. <https://zen-traffic-data.net/english/> .
- He, Z., He, S., Guan, W., 2015a. A figure-eight hysteresis pattern in macroscopic fundamental diagrams and its microscopic causes. *Transportation Letters* 7, 133–142.
- He, Z., Liang, Z., 2017. Visualizing traffic dynamics based on floating car data. *Journal of Transportation Engineering* 143, 04017005.
- He, Z., Lv, Y., Lu, L., Guan, W., 2019. Constructing spatiotemporal speed contour diagrams: using rectangular or non-rectangular parallelogram cells? *Transportmetrica B* 7, 44–60.

- He, Z., Zhang, W., Jia, N., 2020. Estimating Carbon Dioxide Emissions of Freeway Traffic: A Spatiotemporal Cell-Based Model. *IEEE Transactions on Intelligent Transportation Systems* 21, 1976–1986.
- He, Z., Zheng, L., Chen, P., Guan, W., 2017. Mapping to Cells: A Simple Method to Extract Traffic Dynamics from Probe Vehicle Data. *Computer-Aided Civil and Infrastructure Engineering* 32, 252–267.
- He, Z., Zheng, L., Guan, W., 2015b. A simple nonparametric car-following model driven by field data. *Transportation Research Part B: Methodological* 80, 185–201.
- Irani, M., Peleg, S., 1990. Super resolution from image sequences, in: *Proceedings - International Conference on Pattern Recognition*, pp. 115–120.
- Jiang, R., Hu, M.B., Zhang, H.M., Gao, Z.Y., Jia, B., Wu, Q.S., Wang, B., Yang, M., 2014. Traffic experiment reveals the nature of car-following. *PloS one* 9, e94351.
- Laval, J., He, Z., Castrillon, F., 2012. Stochastic extension of newell’s three-detector method. *Transportation Research Record* 2315, 73–80.
- Laval, J., Leclercq, L., 2010. A mechanism to describe the formation and propagation of stop-and-go waves in congested freeway traffic. *Philosophical transactions. Series A, Mathematical, physical, and engineering sciences* 368, 4519–41.
- Ma, X., Dai, Z., He, Z., Ma, J., Wang, Y., Wang, Y., 2017. Learning Traffic as Images: A Deep Convolution Neural Network for Large-scale Transportation Network Speed Prediction. *Sensors* 17, 818.
- Treiber, M., Helbing, D., 2002. Reconstructing the spatio-temporal traffic dynamics from stationary detector data. *Cooper@tive Tr@nsport@* 24, 1–24.
- Treiber, M., Kesting, A., Wilson, R.E., 2011. Reconstructing the Traffic State by Fusion of Heterogeneous Data. *Computer-Aided Civil and Infrastructure Engineering* 26, 408–419.
- Tsai, R., Huang, T., 1984. Multi-Frame Image Restoration and Registration. *Advances in Computer Vision and Image Processing* 1, 317–339.

- U.S. Federal Highway Administration, 2006. The Next Generation Simulation Program (NGSIM). <http://ops.fhwa.dot.gov/trafficanalysistools/ngsim.htm> .
- Wan, Q., Peng, G., Li, Z., Inomata, F.H.T., 2020. Spatiotemporal trajectory characteristic analysis for traffic state transition prediction near expressway merge bottleneck. *Transportation Research Part C: Emerging Technologies* 117, 102682.
- Wang, Y., Papageorgiou, M., Messmer, A., 2007. Real-Time Freeway Traffic State Estimation Based on Extended Kalman Filter: A Case Study. *Transportation Science* 41, 167–181.
- Wang, Y., Papageorgiou, M., Messmer, A., 2008. Real-time freeway traffic state estimation based on extended Kalman filter: Adaptive capabilities and real data testing. *Transportation Research Part A: Policy and Practice* 42, 1340–1358.
- Wang, Y., Papageorgiou, P., 2005. Real-time freeway traffic state estimation based on extended Kalman filter: a general approach. *Transportation Research Part B: Methodological* 39, 141–167.
- Wang, Z., Liu, D., Yang, J., Han, W., Huang, T., 2015. Deep networks for image super-resolution with sparse prior, in: *Proceedings of the IEEE International Conference on Computer Vision*, pp. 370–378.
- Wu, Y., Teufel, B., Sushama, L., Belair, S., Sun, L., 2021. Deep Learning-Based Super-Resolution Climate Simulator-Emulator Framework for Urban Heat Studies. *Geophysical Research Letters* 48, 1–11.
- Zhang, K., Feng, X., Jia, N., Zhao, L., He, Z., 2022. TSR-GAN: Generative Adversarial Networks for Traffic State Reconstruction with Time Space Diagrams. *Physica A: Statistical Mechanics and its Applications* 591, 126788.
- Zhang, Y., Tian, Y., Kong, Y., Zhong, B., Fu, Y., 2018. Residual Dense Network for Image Super-Resolution, in: *Proceedings of the IEEE Computer Society Conference on Computer Vision and Pattern Recognition*, pp. 2472–2481.

Zhang, Z., Wang, Y., Chen, P., He, Z., Yu, G., 2017. Probe data-driven travel time forecasting for urban expressways by matching similar spatiotemporal traffic patterns. *Transportation Research Part C: Emerging Technologies* 85, 476–493.

Zielke, B., Bertini, R., Treiber, M., 2008. Empirical Measurement of Freeway Oscillation Characteristics: An International Comparison. *Transportation Research Record: Journal of the Transportation Research Board* 2088, 57–67.